

# Structural assessment of turbine blades using guided waves

Kena Makaya<sup>1,2</sup>, Kenneth Burnham<sup>1</sup>

<sup>1</sup>Long Range Ultrasonic (LRU) Section, TWI, Granta Park, Great Abington, Cambridge, UK,  
CB21 6AL

Telephone no: +44 (0)1223 899000

E-mail address: kena.makaya@twi.co.uk, kenneth.burham@twi.co.uk,

<sup>2</sup>School of Metallurgy and Materials, University of Birmingham, Edgbaston, Birmingham, B15  
2TT

## Abstract

Wind energy is an increasingly important contributor of power within the renewable energy sector. In recent years there have been an increasing number of reports on defective turbine blades contributing towards turbine failure. Within the larger blade designs, a composite structure of glass fibre re-inforced plastic (GFRP) provides support - termed a *Shear Web* or *Spar Box*. Disbond between the inner shell and bonding flange of the support is not uncommon. Other defects include delamination between the laminate plies that comprise the support structure and structural damage due to impact. Guided Wave Testing (GWT) is a non-destructive testing technique which enables the detection of defects for in-service inspection. This study analyses the propagation of Lamb waves within GFRP laminates, and sandwich structures, based upon elastic properties, plate thickness, fibre-orientation and ply lay-up as well as discontinuities such as delamination, disbond and impact damage. The results of the study will determine the shape of the suggested sensor array based upon mode attenuation and directional velocity.

## 1. Introduction

In February 2009, the United Kingdom (UK) recorded a 38% increase in the total installed capacity (3,331 MW) above 2007 levels, [1]. Furthermore, the UK is now the world leader in offshore wind energy with 598MW capacity. The UK government has set a target to obtain 20% of electricity from renewable sources by 2020 with wind energy expected to be the biggest contributor.

Cost analysis of wind power remains uncertain. Operational and maintenance (O&M) costs for new large turbines are rarely reported. An analysis by Rademakers *et al.*, [2], disclosed that 60% of turbine lifecycle cost comprised component parts, and of those parts, the rotor and the nacelle absorbed 30% of the total cost each. Further analysis on maintenance costs attributed 34% of all downtime to the rotor blade. Although, this provides little more than an indication of the overall O&M costs, it is sufficiently significant to consider non-destructive testing (NDT) for wind-turbine blades.

Typical rotor blades are made from a composite construction of glass fibre, resin (epoxy, acrylic or phenolic) and possibly wood. Such composite materials can be manufactured by a number of techniques combining the fibre and resin into a consolidated product. The fibres may be separate from the resin before manufacture or may already be combined in the form of pre-preg material. The manufacturing technique selected depends partly upon the size and quality of the composite required, [3].

Figure 1 illustrates a typical cross-section view of a blade incorporating a strengthening member known as a *Shear Web* extending from the rotor hub to the tip of the blade.

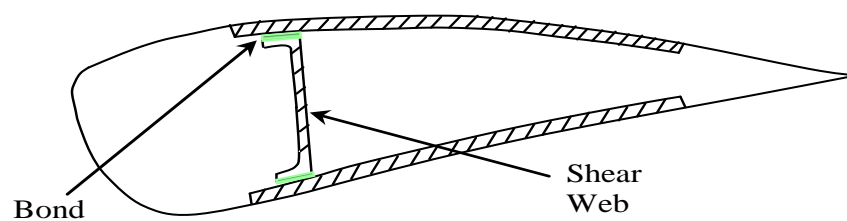


**Figure 1. Rotor Blade cross-section**

Composite materials can be degraded in service by a number of mechanisms dependant upon the environment and the sensitivity of the materials used. The mechanisms of degradation include static overload, impact, fatigue, overheating, lightning strike and creep. However, although the mechanisms by which defects are initiated and grow are varied, only a small number of different types of defect result: fracture or buckling of fibres, failure of the interface between the fibres and matrix, cracks, delaminations, bond failures and ingress of moisture, [4].

Turbine blades are largely inaccessible and thus any inspection area must be suitable for long-term automated monitoring. Although details of blade defects are exceptionally difficult to obtain, blade manufacturers have, on occasion, reported defects involving the shear web. The shear web has a flat vertical structure which bends at each inner blade surface to provide a bonding flange making the structure suitable for siting sensors. Long Range Ultrasonic Testing (LRUT) is an NDT technique which uses low frequency guided waves to inspect pipelines. It is particularly suitable as a tool to inspect large areas such as the shear web. As the technique is relatively new and mainly used for assessing metallic structures (pipes, plates, railway tracks and rods), it has so far had little application to non-metallic materials.

The demand within the industry for larger turbines, and hence increased blade length, creates the drive for improvements in blade technology. A key element of this is to increase monitoring of blade condition throughout their service lives as condition monitoring in this area is relatively immature and failure modes for GFRP are not well documented. Monitoring will enhance knowledge of blade condition, early awareness of degradation and defects and lead to improved management and maintenance of wind turbines, minimising routine operational costs and mitigating against sudden failure. The cost of sudden failure exceeds just the cost of replacing a blade, since additional damage may occur in the gear box and generator and adjacent wind turbines from loose blades. This paper will attempt to analyse guided waves in composite

materials, contained within the rotor blade, and assess how it may contribute to a structural health monitoring system.

## 2. Guided waves

In plate-like structures (where material thickness is comparable to the ultrasound wavelength) it is possible to propagate guided waves (Lamb waves) parallel to the plate surfaces. Lamb waves travel through the entire thickness of the material and can propagate for considerable distances in plates thus making it possible to detect flaws over a sizable area with a single transducer (or pair of transducers). For a plate of given thickness and frequency, there always exist a finite number of symmetrical and anti-symmetrical Lamb waves, each differing from the other by their phase and group velocities and distribution of the displacements and stresses throughout the thickness of the plate [5]. A typical mode distribution plot, showing variation of modal phase velocities as a function of frequency is illustrated in Figure 2.

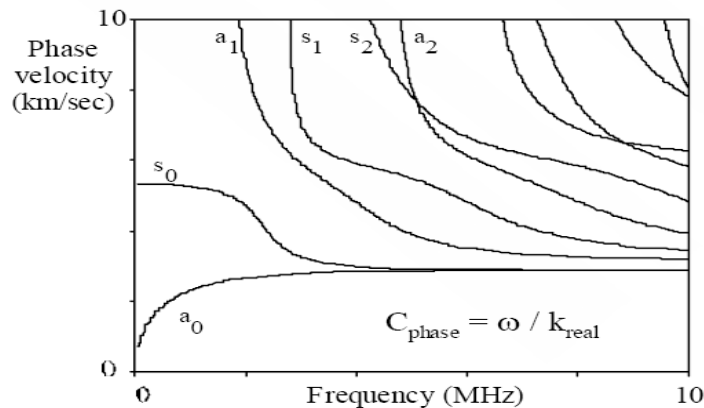


**Figure 2. Phase velocity versus frequency for normalized plate thickness**

Different types of defect will typically exhibit different characteristics thus providing a potential mechanism for discrimination. Considering the propagation of such signals in a rotor blade structure, it is vitally important to note that the effects of the material boundaries will have a major impact on the nature of the energy propagation. Typically, guided ultrasonic wave modes will be established, and in order to predict the nature of the output waveform monitored by the reception transducer, it is important to understand the multimode and dispersive properties of such waves within a specific material.

A significant issue in employing guided wave propagation in composite material inspection lies in the lossy characteristics of the materials and attenuation effects are often a significant limiting factor to the application of any ultrasonic based inspection technique. Attenuation effects can broadly be sub-divided into the following categories:

- reduction in signal amplitude due to dispersion
- physical energy loss mechanisms
- material geometrical effects e.g. anisotropic properties

Dispersion can be controlled by careful selection of propagating mode. Physical energy loss through material damping and viscoelastic effects, is material and frequency dependent (increasing rapidly with frequency) and can be addressed through control of excitation (and/or monitored) frequency band. Effects due to the anisotropic nature of typical composite materials may involve energy being guided in unexpected (and possibly unwanted) directions due to the lay-up of the material.

### 3. Experimental results

Three GFRP laminate samples were investigated with varying laminar lay-up. Details are provided in Table 1.

**Table 1. Samples specifications**

Sample	Type	Dimensions (mm)	Fibre Orientation	Manufacture Method	Defects
1	Laminate Glass Fibre	1300x1000x7.4	0°/90°	Autoclave	None
2	Laminate Glass Fibre	2000x1000x4	0°-90°/±45°	Autoclave	None
3	Sandwich Balsa Wood	2000x1000x14	0°-90°/±45° (Top & bottom surfaces)	Autoclave	None

### 3.1 Bi-directional sample

Sample 1 is a  $0^\circ/90^\circ$  bi-directional GFRP laminate plate which was investigated in the laboratory of Kaunas Technology University (KTU - project partners). The experiment was carried out using a low frequency ultrasonic measurement system (UTRALAB) combined with an automatic stepper comprising a single axis scanner and adjustable transducer holders. The transducers were PZT type and were coupled to the structure using glycerol. The experimental set-up, featuring a pitch-catch technique, is shown in Figure 3.

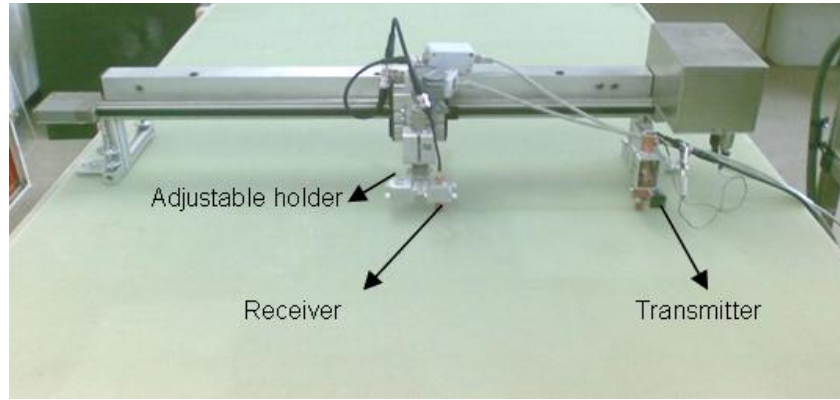


**Figure 3. Experimental set-up (courtesy of KTU)**

The signal details were: a Hann-windowed 100KHz sine-wave with amplitude  $100V_{PP}$  and gain 10dB. The tests were performed such that the line directly connecting the transmitter to the receiver was initially parallel to the on-fibre ( $0^\circ$ ) direction, and then perpendicular to the on-fibre direction i.e. maximally off-fibre ( $45^\circ$ ). The fixed transmitter was placed with a maximum displacement of 250 mm from the initial receiver position. The receiver was then incrementally moved towards the transmitter in steps of 1 mm completing a distance of 200mm. The data was subsequently analysed using MatLab where a signal processing technique, two-dimensional Fast Fourier Transform (2DFFT), was used to ascertain which Lamb wave modes were propagating within the GFRP sample. The 2DFFT assumes that the surface function has been sampled in the x dimension with sample interval  $T_x$  and sampled in the y dimension with sample interval  $T_y$ . The resulting sampled 2DFFT function is  $h(pT_x, qT_y)$  where  $p=0,1,\dots,N-1$  and  $q=0,1,\dots,M-1$ , [6], (1):

$$H\left[\frac{n}{NT_x}, \frac{m}{MT_y}\right] = \sum_{q=0}^{M-1} \sum_{p=0}^{N-1} h[pT_x, qT_y] e^{-j2\pi\left(\frac{mq}{M} + \frac{Np}{N}\right)}$$

Contour plots in the wave-number ( $k$ ) and frequency-thickness ( $ft$ ) domain were subsequently analysed. The different wavenumbers provide information on the mode content of signals. Figure 4 illustrates a contour plot for the off-fibre ( $45^\circ$ ) direction and Figure 5 illustrates a contour plot for the on-fibre ( $0^\circ$ ).

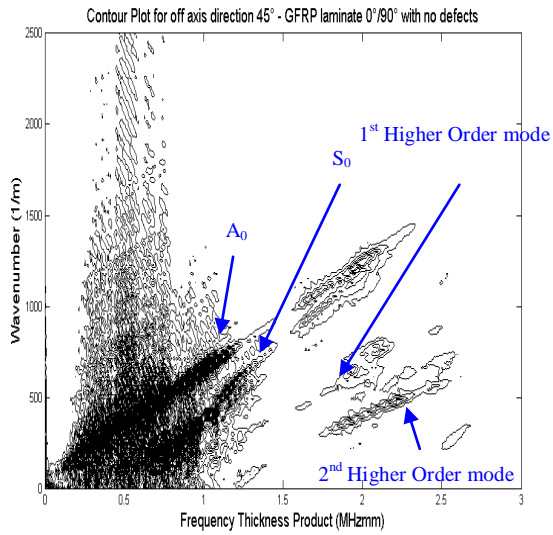


**Figure 4. Contour plot for off-fibre (45°)**

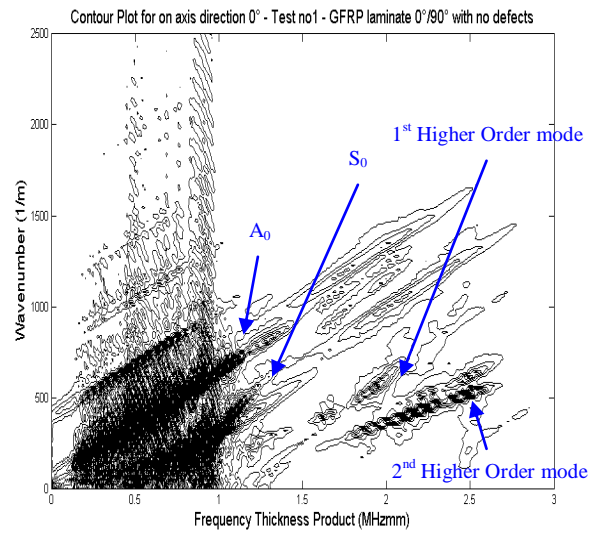


**Figure 5. Contour plot for on-fibre(0°)**

Converting into the phase velocity-frequency thickness domain, the dispersion curve for the on-fibre (0°) capture is illustrated in Figure 6.

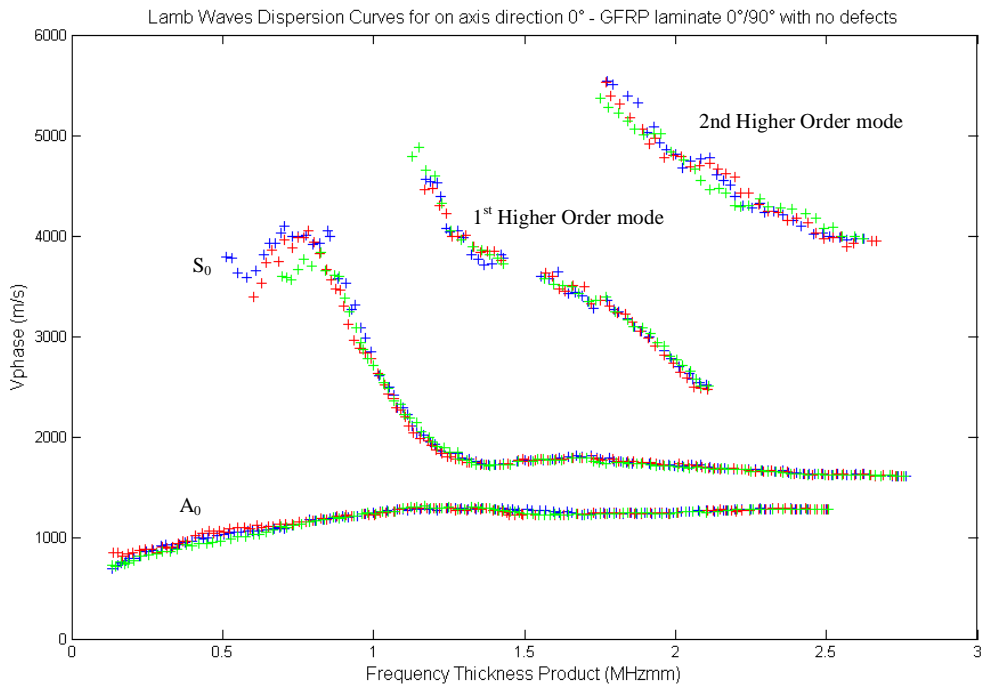


**Figure 6. Dispersion curves for on axis direction 0° - GFRP laminate 0°/90° with no defects**

Three traces are shown (blue, red, green) representing three individual tests to ensure the results were repeatable. Four wave modes were observed: the fundamental modes,  $S_0$  and  $A_0$ , and two higher order modes.

Figure 7 and Figure 8 illustrate a direct comparison between on and off-fibre tests for the fundamental modes and higher order modes respectively.

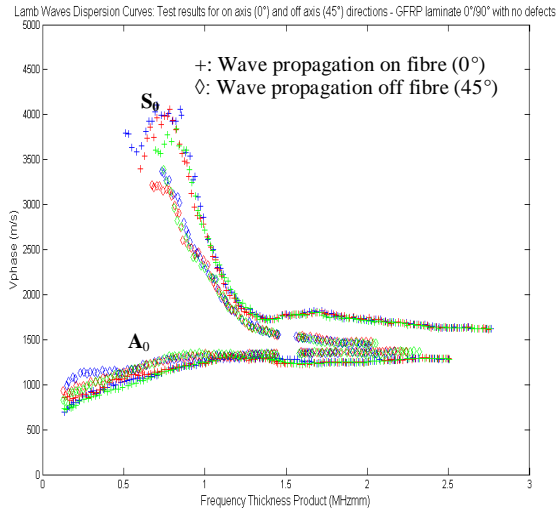


**Figure 7.  $S_0$  and  $A_0$  for on and off-fibre propagation**

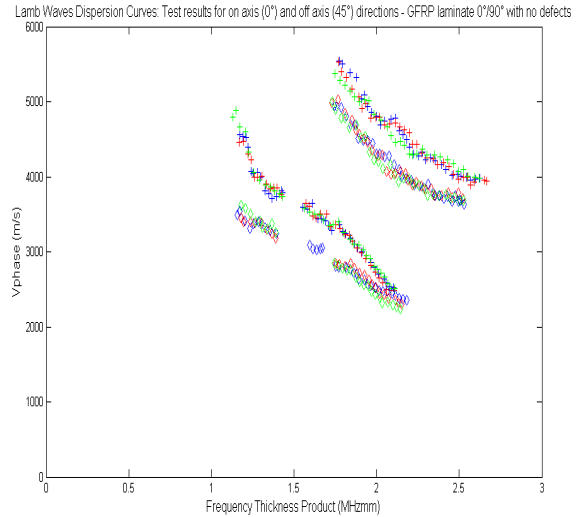


**Figure 8: Higher order modes for on and off-fibre propagation**

It may be observed in

Figure 7 that there is little difference between the  $A_0$  mode dispersion curves for on-fibre ( $0^\circ$ ) and off-fibre ( $45^\circ$ ) directions. However, the phase velocities for the  $S_0$  modes show some dependence upon fibre-direction where the dispersion curves appear to diverge for signals above  $1.4\text{MHzmm}$ . There also appears to be a loss of modal energy for the off-fibre ( $45^\circ$ ) direction centred at  $1.5\text{MHzmm}$ . The phase velocities for the higher order modes also appear to depend upon fibre-orientation.

### 3.2 Quasi-isotropic sample

Sample 2, a quasi-isotropic, non-defective GFRP laminate, was compared with Sample 1 to analyse the effects of fibre-orientation on the propagating modes. The sample dimensions were 2000mm x 1000mm x 4mm with a ply lay-up as follows:

- Woven ( $0^\circ/90^\circ$ )
- Biaxial ( $\pm 45^\circ$ )
- Woven
- Woven
- Biaxial
- Woven

Figure 9 illustrates the presence of just the fundamental wave modes for the quasi-isotropic plate whilst Figure 10 shows that additional higher order modes are present in the bi-directional plate. It is further evident that greater detail of the  $S_0$  mode exists for the bi-directional sample than does for the quasi-isotropic sample. The fundamental modes in the bi-directional sample are present up to 2.5MHzmm whereas detail for these modes in the quasi-isotropic sample is limited to 1.2MHzmm.

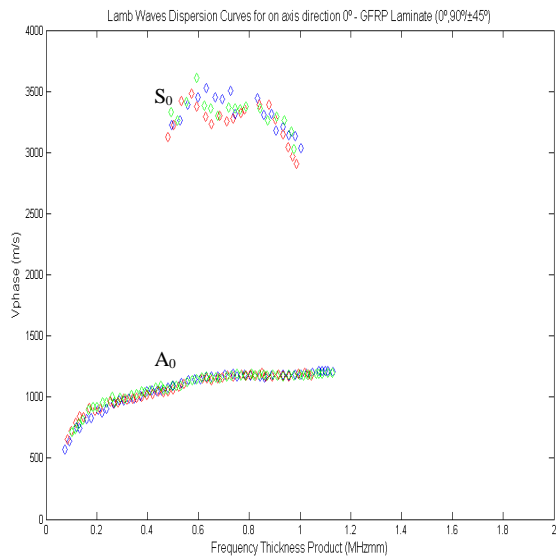


**Figure 9.  $S_0$  and  $A_0$  for quasi-isotropic sample ( $0^\circ$ ,  $90^\circ/\pm 45^\circ$ )**

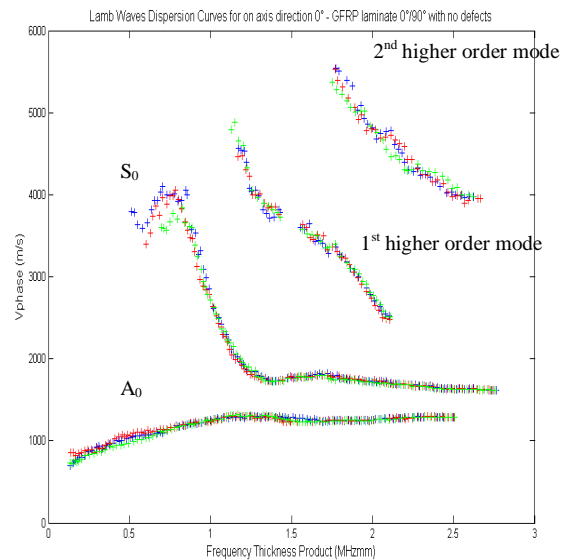


**Figure 10: Wave modes for bi-directional sample ( $0^\circ/90^\circ$ )**

### 3.3 Sandwich structure - GFRP/balsa wood/GFRP

Sample 3, a composite plate comprising a sandwich structure of GFRP (14mm):Balsa-wood (6mm):GFRP (4mm) was analysed to directly compare the mode propagation of ultrasound waves with Sample 2 - the 4mm GFRP laminate representative of the sandwich outer layers. The dimensions of Sample 3 were 2000mm x1000mm x 14mm. The experimental set-up remained unchanged.

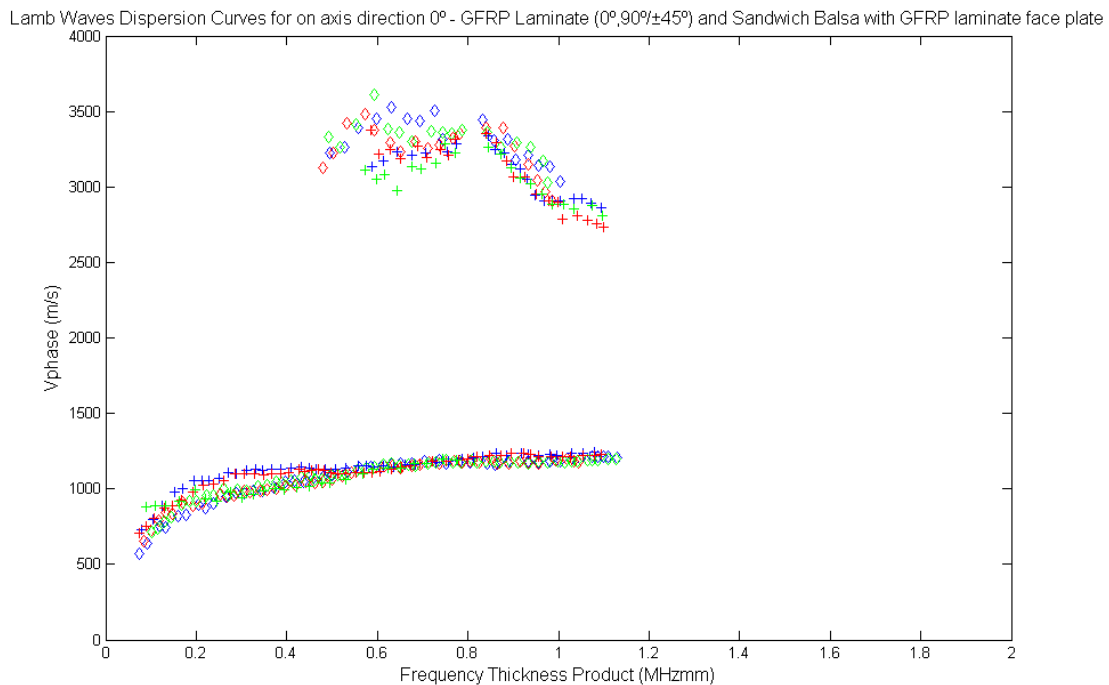


**Figure 11. S<sub>0</sub> and A<sub>0</sub> mode propagation in GFRP laminate (◇) and sandwich structure (+)**

Figure 11 compares the dispersion curves of the GFRP laminate with the sandwich structure. It can be observed that little difference exists between the A<sub>0</sub> modes of each sample which are almost identical for frequency-thickness values above 0.5MHzmm. Between the range 0.2MHzmm and 0.4MHzmm, there is a slight divergence between the two plots; however, both plots converge for frequency-thickness values below 0.2MHzmm. Similarly, the S<sub>0</sub> modes for each sample are almost identical above 0.8MHzmm with a little divergence between the two plots below this value.

## 4. Discussion

The propagation modes for the bi-directional plate (Sample 1), Figure 7 and Figure 8, illustrated a loss of energy for the fundamental modes centred at approximately 1.5MHzmm for the off-fibre (45°) test-scan. The on-fibre (0°) test-scan showed no such loss of energy for the fundamental modes. It could be that this loss of modal energy may be attributed to the resonance frequency of the plate.

Sample 1 comprised 16 plies each 0.46mm thick (sample thickness 7.4mm). If the centre-frequency of the energy gap is normalised:

$$\frac{1.5\text{MHz}}{7.4\text{mm}} = 202.703\text{KHz}$$

The phase velocity for the  $S_0$  mode at 1.5MHzmm is 1600m/s and the phase velocity for the  $A_0$  mode at 1.5MHzmm is 1400m/s. Evaluating the wavelength for both modes:

$$\lambda_{(S_0)} = \frac{1600 \text{ m/s}}{202.703 \text{ KHz}} = 7.8\text{mm} \quad \lambda_{(A_0)} = \frac{1400 \text{ m/s}}{202.703 \text{ KHz}} = 6.9\text{mm}$$

Thus, it is observed that the wavelengths for both  $A_0$  and  $S_0$  modes are remarkably similar to the thickness of the sample which may result in some form of resonance.

Laminar lay-up also has an affect on the dispersion curves. The quasi-isotropic plate (Figure 9) illustrated the presence of only the fundamental modes which extended up to 1MHzmm and 1.2MHzmm for the  $S_0$  and  $A_0$  modes respectively. Figure 10, for the bi-directional plate, featured higher order modes in addition to the fundamental modes where the  $S_0$  and  $A_0$  modes extended up to 2.8MHzmm and 2.5MHzmm respectively. Thus, more modal detail exists for the bi-directional plate. The fibre volume for both plates is 50%. Whilst both plates have different thickness dimensions - 7.4mm for the bidirectional plate and 4mm for the quasi-isotropic - it is possible that the fibre orientation in the quasi-isotropic plate has increased the level of scattering and thus lowered the signal to noise ratio (SNR). Research on microcracks in composite materials by Djordjevic recorded reduced velocity and scattering at specific frequencies [7]. In addition, the laminar lay-up for the quasi-isotropic plate is not symmetrical: there are more instances of fibres orientated along the 0°/90° direction than fibres orientated along the ±45° direction.

Finally, the dispersion curves for Sample 3 (sandwich plate) were compared with the quasi-isotropic laminate plate which forms the top and bottom layers of the sandwich plate. Figure 11 illustrated that the dispersion curves for each sample are strikingly similar. It may be that during the test for the sandwich plate, the Lamb waves were propagating only in the outer GFRP layers. Further investigation and analysis is required.

## **5. Conclusion**

The strategic importance of monitoring wind turbine blades has been highlighted, with emphasis placed on the economic benefits associated with preventative failure. Significant challenges exist in using guided wave techniques to monitor the primary blade structures due to the common use of composite materials (in particular GFRP). The inherent anisotropy of the laminar lay-up and inconsistent manufacturing processes significantly increase the levels of attenuation and scatter. This results in difficulties generating and propagating specific wave modes. However, this research has indicated that specific modes can be identified which may be used for testing different parts of a rotor-blade, specifically for the shear web structure.

Further research is required to analyse the effects on different modes when defects such as delamination, debonding and impact damage are introduced into the material. Present work includes the design of an array for mode detection using TWI's low-frequency ultrasonic Teletest<sup>®</sup> Focus system.

## Acknowledgements

Kena Makaya is studying for an Engineering Doctorate at the University of Birmingham under the sponsorship of EPSRC and TWI Ltd. The work was carried out under the 'In-situ Monitoring of on- and offshore Wind Turbine Blades Using Energy Harvesting Technology' project, which is funded by the European Commission within the Framework 7 Programme.

The experimental work was carried out in collaboration with Kaunas Technology University (KTU).

## References:

- <sup>1</sup> Executive Committee for the Implementing Agreement for Co-operation in the Research, Development, and Deployment of Wind Energy Systems of the International Energy Agency, 'IEA Wind Energy Annual Report 2005', IEA, 2006
- <sup>2</sup> L.W.M.M. Rademakers *et al.*, 'Assessment and Optimisation of Operation and Maintenance of Offshore Wind Turbines', ECN Wind Energy, [http://www.ecn.nl/docs/dowec/2003-EWEC-O\\_M.pdf](http://www.ecn.nl/docs/dowec/2003-EWEC-O_M.pdf)
- <sup>3</sup> D. Hull, T.W. Clyne, D.R. Clarke, and S. Suresh, "An Introduction to Composite Materials" Cambridge Solid State Science, 1996.
- <sup>4</sup> "Characterization, Analysis and Significance of Defects in Composite Materials", AGARD Conference Proceedings No. 355, 1983.
- <sup>5</sup> I.A. Viktorov, "Rayleigh and Lamb Waves – Physical Theory and Applications", Plenum Press, 1967.
- <sup>6</sup> E.O.Brigham, 'The Fast Fourier Transform And Its Applications', Prentice Hall Signal Processing Series, 1988, Chapter 2, pp233
- <sup>7</sup> DJordjevic BB, 'Ultrasonic Characterisation of Advanced Composite Materials', the 10<sup>th</sup> International Conference of the Slovenian Society for Non-Destructive Testing, September 1-3, 2009, 47-57.

